Available online at www.sciencedirect.com
SCIENCE DIRECT
Polymer 46 (2005) 1935–1942
polymer
www.elsevier.com/locate/polymer

Crystallographic texturing in single poly(*p*-phenylene benzobisoxazole) fibres investigated using synchrotron radiation

R.J. Davies[a,*], S.J. Eichhorn[a], C. Riekel[b], R.J. Young[a]

[a]*Manchester Materials Science Centre, UMIST/University of Manchester, Grosvenor St, Manchester M1 7HS, UK*
[b]*European Synchrotron Radiation Facility, B.P. 220, F-38043, Grenoble Cedex, France*

Received 17 June 2004; received in revised form 30 November 2004; accepted 17 December 2004
Available online 18 January 2005

Abstract

A micro-focus synchrotron beam has been used to investigate crystallographic texturing in poly(*p*-phenylene benzobisoxazole) fibres. By generating diffraction patterns across single fibres, it is possible to produce profiles showing scattering intensity as a function of beam position across the fibre. A straightforward model has been developed to allow the degree of texturing to be quantified for direct comparison between fibre types. The experimental results are found to fit a radial fibrillar-texturing model, which incorporates a distribution in radial orientation about the fibre axis. Previous studies reporting the *a*-axis of the PBO unit cell to be aligned radially within fibrils about the fibre axis are found to be correct.

The degree of radial fibrillar texturing is in the same fibre order as tensile modulus and crystalline domain orientation for PBO fibres with different processing histories. It is proposed that the degree of radial fibrillar texturing is therefore related to fibre homogeneity. An extrapolation of tensile modulus to that of a perfectly homogeneous fibre results in a value in good agreement with the PBO crystal modulus. This further supports the proposal that the degree of radial fibrillar texturing is related to fibre homogeneity.

Keywords: PBO; WAXS; Radial fibrillar texturing

1. Introduction

Poly(*p*-phenylene benzobisoxazole), or PBO, is a high-performance semi-crystalline polymeric fibre. It belongs to a group of materials known as 'rigid-rods' that are characterised by a high degree of molecular chain conformation. The polymer backbone of PBO may be considered as consisting of a series of highly-oriented and rigid molecules. It is this structural feature that is largely responsible for the remarkable tensile properties reported for this fibre type [1–3]. PBO was first developed as part of the US Air Force's Ordered Polymer Programme and is now produced by Toyobo (Japan) under the tradename Zylon® [4,5]. The polymer repeat unit of PBO is shown in Fig. 1 [6].

There are two varieties of PBO available commercially, as-spun (AS) and high-modulus (HM). Both of these fibre types are manufactured from a nematic dope using a dry-jet wet-spinning process and coagulated in an aqueous solution [1,4–9]. Whereas PBO AS is only tension dried, the HM fibre type undergoes a subsequent heat-treatment process. This involves heating the fibre to a high temperature during tension application [4,7]. The result is a fibre with a higher modulus than that of PBO AS. An ultra-high modulus PBO variety (HM+) is also currently under development by Toyobo (Japan) [7,10]. This is produced using a non-aqueous coagulation system, resulting in a more homogeneous fibre. The HM+ variety therefore exhibits a significantly higher tensile modulus than that of PBO HM [10].

Previous synchrotron wide-angle X-ray scattering (WAXS) studies of PBO have investigated various aspects of its crystallographic structure [11,12]. These studies report PBO to be highly crystalline with a high degree of domain orientation with respect to the fibre axis [11,12]. A recent study has also examined skin-core differences in crystalline domain orientation and crystal strain [13]. This was possible

* Corresponding author. Tel.: +33 476 88 2961; fax: +33 476 88 2904.
E-mail address: rdavies@esrf.fr (R.J. Davies).

0032-3861/$ - see front matter © 2004 Elsevier Ltd. All rights reserved.
doi:10.1016/j.polymer.2004.12.031

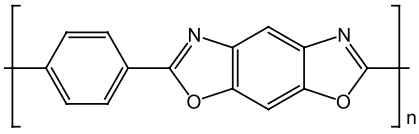

Fig. 1. Polymeric repeat unit of the PBO fibre type [6].

through the use of a micro-focus synchrotron beam to generate diffraction patterns across single fibres [13]. An interesting feature of such across-fibre WAXS experiments is the variation in the relative intensities of equatorial reflections as the beam position changes across the fibre diameter. These variations are demonstrated in Fig. 2 as a series of radial intensity profiles for the most intense PBO equatorial reflections. When the edge of the fibre is positioned in the beam, diffraction intensity associated with the 010 reflection is significantly greater than that of the 200 reflection. Conversely, when the centre of the fibre is positioned in the beam, the 200 reflection exhibits greater intensity than the 010 reflection. Such intensity variations have been reported previously in other high-performance fibres such as poly(*p*-phenylene terephthalamide) or PPTA [14,15]. They are attributed to radial crystallographic texturing within the fibre structure [14,15].

Crystallographic texturing, similar to that in PPTA, has also been reported previously in the PBO fibre type [1,16,17]. From the variations in across-fibre scattering intensity, Kitagawa et al. deduced that the *a*-axis of the PBO unit cell is oriented radially around the fibre axis [1]. This observation was possible through the use of localised diffraction techniques such as selected-area electron diffraction (SAED) [1,16,17]. However, whilst such techniques are capable of identifying the existence of crystallographic texture, they are not ideal for such studies. This is primarily due to the extensive sample preparation required, such as the requirement of ultra-thin sectioning. This risks the introduction of artificial texture. By contrast, synchrotron diffraction can be performed in transmission on single (un-sectioned) fibres. This makes it well suited for crystallographic texture analysis.

The study of crystallographic texturing requires the use of a beam diameter that is considerably smaller than the diameter of the fibre under study [18]. The preferred method of X-ray-based texture analysis is therefore a micro-focused synchrotron beam [18]. Investigations of fibre texture using synchrotron radiation have previously been performed on polyethylene, PPTA and carbon fibres [14,18,19]. In PPTA (Kevlar^{49}) for example, there are thought to be a continuous rotation of sheets with the *b*-axis of the unit cell oriented radially [14]. Such crystallographic texturing is termed radial fibrillar texturing (RFT) due to the radial arrangement of crystallographic planes within fibrils around the fibre axis. An idealised RFT model is shown in Fig. 3. For PPTA the idealised model does not fully agree with experimental findings [14]. This is thought to be due to an orientation distribution around the fibre axis [14]. Indeed, a relatively recent study of texturing in PPTA using micro-focused synchrotron radiation has successfully modeled RFT using a Monte-Carlo approach [15]. Whilst this is again based around the idealised model, it also incorporates an orientation distribution [15].

This study reports on crystallographic texturing in the three PBO fibre varieties, AS, HM and HM+. Differences in the degree of texturing between the different fibre types can therefore be assessed. Such differences may be related directly to variations in the fibre production process.

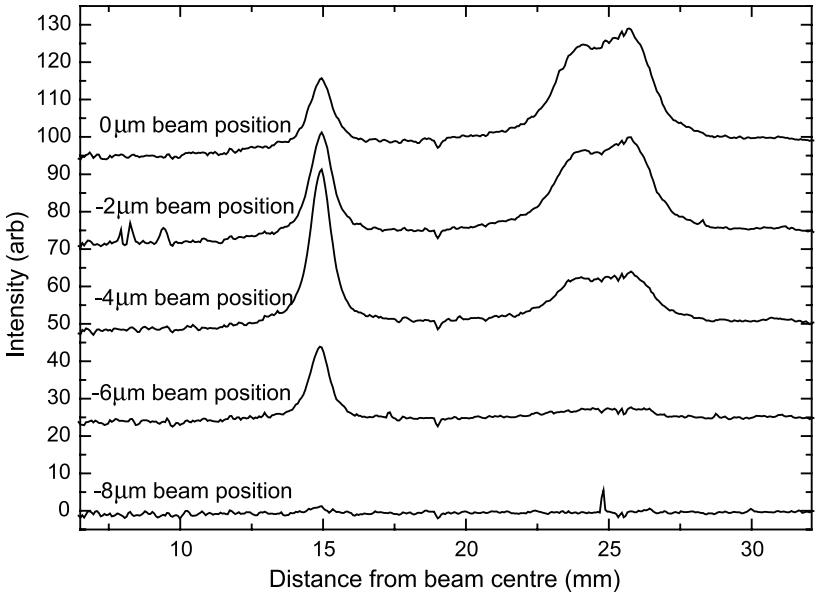

Fig. 2. Radial profiles (offset) of PBO HM equatorial reflections at different beam positions across the fibre (where 0 μm = fibre centre position).

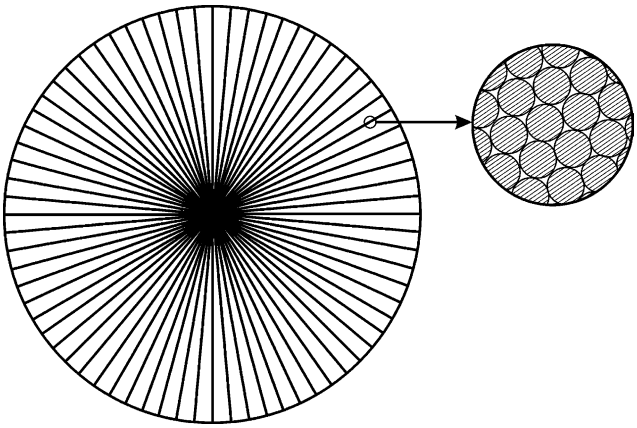

Fig. 3. Approximation of ideal radial fibrillar texturing.

Furthermore, the relationships between crystallographic texture and other fibre parameters such as tensile modulus can be considered. A straightforward modelling approach is employed in order to determine a quantitative measure of crystallographic texturing. The value of such a model has already been demonstrated for PPTA [14,15] and allows for comparisons to be made between this and previous studies [14].

2. Experimental

2.1. Materials

Three varieties of PBO have been investigated within this study, as-spun (AS), high-modulus (HM) and ultra-high-modulus (HM+). The AS and HM fibre types are commercially available under the trade-name Zylon® and have been coagulated using an aqueous system [1,4–9]. Whereas the AS fibre is commercialised literally as-spun, the HM fibre undergoes a subsequent heat-treatment process [4,7]. The HM+ fibre is a development variety of PBO and is manufactured using a modified coagulated system [7,10]. This fibre type is also heat-treated. All three varieties of PBO were supplied by Toyobo (Japan).

2.2. Micro-beam wide-angle X-ray scattering (μWAXS)

μWAXS of all samples was carried out at the European Synchrotron Radiation Facility (ESRF) on the micro-focus beamline (ID13). The beamline was configured with glass capillary optics and aperture resulting in an on-sample beam spot-size of approximately 3 μm. A detailed account of the beamline configuration and experimental protocol is reported elsewhere [20]. Diffraction pattern analysis was performed using a combination of the Fit2D software application [21,22] and a custom-written application for batch file processing, peak fitting and integration. Prior to analysis, a background file was subtracted from the data to reduce the air scattering contribution. The radial positions of maximum scattering intensity were then determined for the main equatorial reflections. Total scattering intensities were calculated by the integration of Lorentz IV functions fitted to azimuthal intensity profiles around 180° of these radial positions. The same procedure was applied to both diffraction pattern hemispheres to provide an average value and the procedure repeated for each equatorial reflection in each diffraction pattern for each fibre. All PBO reflections within this study have been indexed according to Fratini et al. [23].

2.3. Theoretical basis of intensity modelling

A straightforward model has been developed in order to quantify the degree of RFT in the different PBO fibre varieties. The model is based upon an idealised structure, as shown in Fig. 3. For any given crystal plane, diffraction will only occur when the Bragg condition is satisfied. Assuming a radial orientation of crystal planes around the fibre axis, diffraction angle (θ) will only satisfy the Bragg condition along one particular fibre radii. Thus diffraction only occurs along so-called 'planes of maximum scattering'. The angular offset between any given plane of maximum scattering and the beam direction (taken as 0°) is denoted Φ. From the positions of the equatorial reflections on the diffraction pattern, and simple geometry, the diffraction angle (θ) can be calculated. Angle Φ may therefore also be calculated based upon a combination of this diffraction geometry, and the fixed angular relationships between crystal planes and unit cell axes.

It has already been reported from the SAED of PBO that the *a*-unit cell axis is radially orientated about the fibre axis [1]. This would therefore correspond to a radial orientation of crystal planes along the [010] direction of the unit cell. These crystal planes give rise to the 010 equatorial reflection. Their diffraction angle must be equivalent to the angle of the plane of maximum scattering (i.e. $\Phi = \theta$). For the PBO HM fibre type this is found to be 8.29° ($\Phi = \theta = \pm 8.29°$). As the PBO unit cell angle $\gamma = 101.3°$, the (200) crystal planes are assumed to be oriented 101.3° from any given fibre radii. For the 200 reflection of PBO HM, the diffraction angle θ is found to be 5.06°. The planes of maximum scattering for the 200 reflection therefore occur at $\Phi = \pm 106.36°$ and $\Phi = \pm 96.24°$ from the incident beam. A clarification of these angular relationships are shown schematically on a fibre cross-section in Fig. 4.

Until this point, RFT has been discussed on the basis of the idealised model shown in Fig. 3. However, for PPTA fibres it has been observed that such a model does not fit the experimental results [14]. The disparity between the idealised model and experimental results may be explained by a distribution in crystalline domain orientation about the fibre axis [14]. A recent study of PPTA corroborates this conclusion, proposing a model which includes a distribution with a constant rotational angle across the fibre radius [15]. The ability of this model to fit experimental data provides a

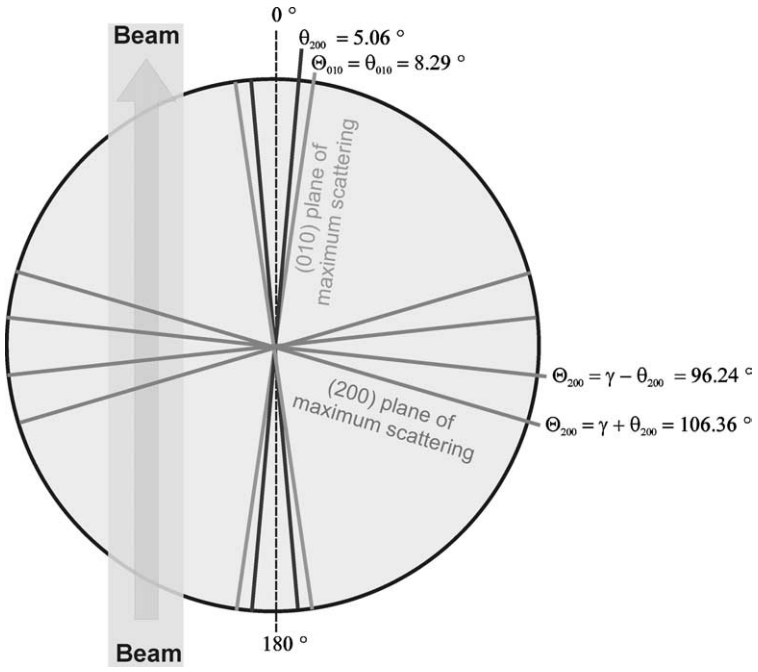

Fig. 4. Clarification of the angular positions of the (200) and (010) planes of maximum scattering for PBO.

sound basis for the application of a similar model to the results presented within this study. With such a distribution, diffraction intensity from a specific crystal plane is still maximised along a plane of maximum scattering. However, other crystallites that are not directly on this plane may also contribute towards diffraction intensity. This may be considered as a rotational disorder of crystallites within the fibre.

2.4. Model implementation

The proposed model assumes fibre homogeneity in the fibre axis direction and radial symmetry about the fibre axis. The fibre is defined within a numerical matrix (I) of m rows and n columns. Each element may be considered as a collection of crystallites from which diffraction may or may not occur. The contribution to total diffraction intensity for each element is determined solely by the angular offset of the element from the beam axis. The intensity contribution of all elements at angle Φ (the plane of maximum scattering) is considered to be 100%. For angular positions other than Φ, the intensity contribution is calculated based upon a Gaussian distribution. Hence it is assumed that the RFT distribution is Gaussian in nature. The intensity contribution for any given element ($I_{(mn)}$) within the model fibre diameter can be calculated using Eq. (1).

$$I_{(mn)} = \exp\left(\frac{\tan^{-1}\left(\frac{n^*}{m^*}\right) \pm \Phi}{\mathrm{FWHM}}\right)^2 \quad (1)$$

where n^* and m^* are the positions of the element relative to the fibre centre and FWHM is the full-width at half-maximum of the Gaussian distribution in RFT. The total diffraction intensity (I_p) for a given beam position (p) is the sum of the intensity contributions from each element within the model gauge area. The model gauge area encompasses all elements along the column vectors within the model beam diameter. This is given by Eq. (2).

$$I_p = \sum_{m=p+B_r^{mod}}^{m=p-B_r^{mod}} \sum_{n=x}^{n=1} I_{(mn)} \quad (2)$$

where B_r^{mod} is the model beam radius which is scaled relative to the model fibre diameter and x is the number of elements in a complete transverse of the matrix. By performing successive calculations of intensity across the modelled fibre, the variation in modelled diffraction intensity with beam position can be determined. The model step size between beam positions is scaled proportionally to the experimental offset between diffraction patterns. Through an iterative process, the FWHM of the RFT distribution is optimised to the experimental data. A beam offset parameter is also incorporated into the model to allow for differences between the central beam position ($p=0$ μm) and the geometrical centre of the fibre.

For RFT modelling, the selection of equatorial reflections must be considered carefully. As the angular relationships between crystal planes are fixed according to unit cell geometry there should be no difference in the distribution in RFT measured between different reflections. However, due to the intensity overlap between the 010 and

$\bar{2}10$ reflections for PBO, the 200 reflection is favoured for determining the degree of RFT. For this reason, model calculations reported within this study are confined to the 200 reflection.

This model simplifies fibre morphology in order to express the degree of orientation in RFT as a single FWHM value. This is an advantage over more complex models [15] as it returns a single value for direct comparison between fibre types. Before considering the results however, the assumptions of the model and their consequences require consideration. The assumption of fibre homogeneity along the fibre axis is not thought to be significant due to the relatively large beam diameter compared to individual crystallite size. Similarly, the fact that the model neglects absorption effects can be justified due to the small sample volumes under study and the low density of PBO fibre. The assumption of radial homogeneity about the fibre axis (fibre symmetry) is more significant. This precludes any possible differences arising from fibre processing (such as variations between skin-core structure for example). A previous study of PPTA fibres reports that such variations need to be included for a good correlation between the model and experimental results [15]. The fact that such parameters are not utilised in this study can be attributed to experimental differences [15]. The previous study used waveguide optics to give a lateral beam dimension of approximately 0.2 μm [15]. The experimental results would therefore be more sensitive to any structural variations. The use of a 3 μm beam in this study reduces these differences through averaging. Furthermore, the inclusion of more variables for model fitting may not necessarily be beneficial in this case where a single FWHM for comparison between fibre types is preferred.

3. Results

3.1. General results

Fig. 2 clearly demonstrates the existence of texturing in the PBO fibre type. However, whilst this method of presentation emphasises across-fibre variations in reflection intensity, it is not suited to investigating differences between fibre types. A more appropriate comparison is therefore shown in Fig. 5.

In Fig. 5, integrated reflection intensity is plotted in a single data series against beam position for the 200 and 010 equatorial reflections. The results show that all three varieties of PBO exhibit evidence of RFT. This can be concluded from the variation in reflection intensity with beam position. This is most apparent for the 200 reflection, which has two intensity maxima across the fibre width. Furthermore, it is possible to observe differences in the degree of RFT between fibre types. The across-fibre intensity variations are much greater in the PBO HM+ fibre type compared to the HM type. Similarly, PBO HM exhibits a greater variation in 200 reflection intensity across the fibre width compared to that of the AS fibre type. This preliminary result suggests that the degree of RFT is in the same fibre order as crystalline domain orientation and fibre modulus [11,13]. Thus both the heat treatment process and the non-aqueous coagulation method used in the production

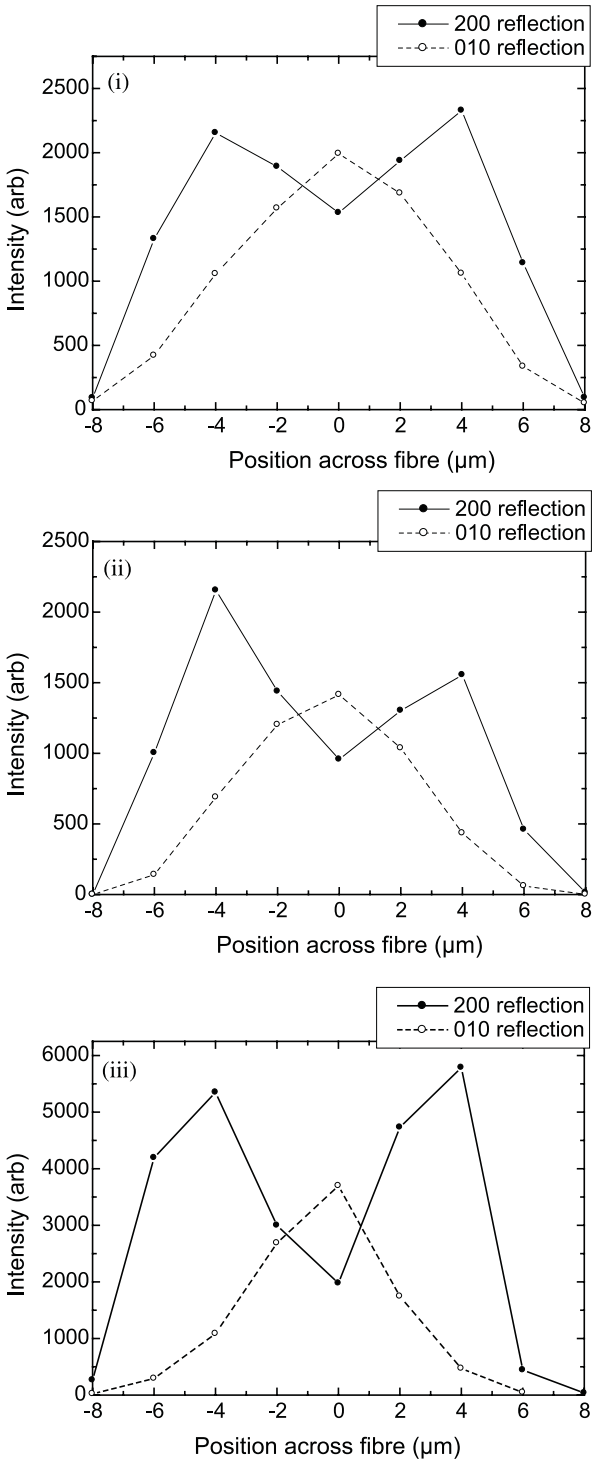

Fig. 5. Variation of integrated intensity of the 200 and 010 reflections across the fibre for (i) PBO AS, (ii) PBO HM and (iii) PBO HM+.

of the HM+ fibre type lead to an increase in the degree of RFT.

This discussion has only considered the 200 reflection of PBO. It is not necessary to consider other equatorial reflections due to the fixed angular relationships between crystal planes. Furthermore, discussions limited to the 200 reflection are more favourable as there exists an intensity overlap between the 010 and $\bar{2}10$ reflections.

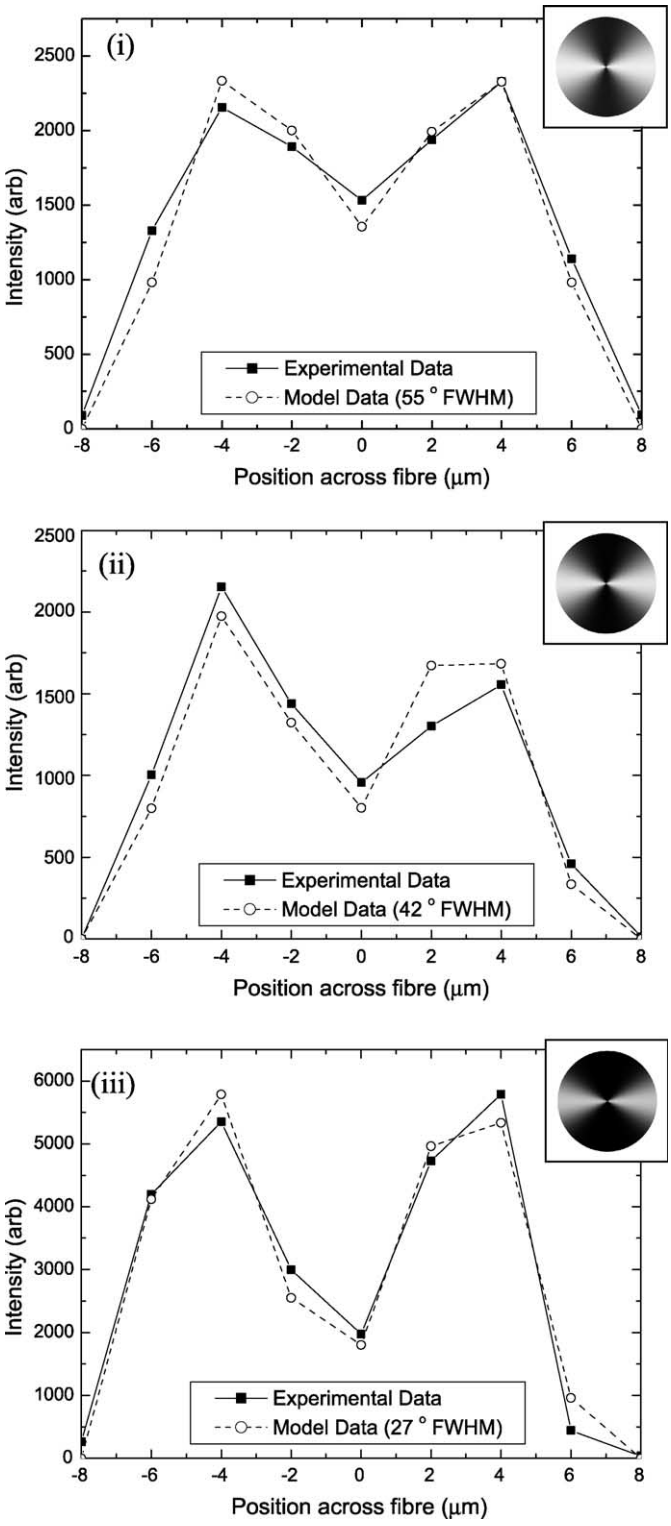

Fig. 6. Comparison of across-fibre (modelled) intensity variations against experimental results and (inset) visual comparison of the distribution in 200 diffraction intensity from modelling of (i) PBO AS, (ii) PBO HM and (iii) PBO HM+.

Table 1
Comparison of parameters yielding best model fit to experimental data for PBO AS, HM and HM+

	Beam offset for model (μm)	Diffraction angle for (200) crystal planes (θ°)	FWHM distribution in RFT (°)
PBO AS	0.0	5.07	55
PBO HM	−0.35	5.06	42
PBO HM+	−0.7	5.08	27

3.2. Intensity modelling

Fig. 6 shows the calculated variation of (200) diffraction intensity across the fibre using the proposed model. The corresponding experimental data is also shown to allow for direct comparison. Also shown on Fig. 6 are visualisations of the model data, inset on each plot. These show the contribution towards diffraction intensity of each volume element within the different PBO fibre types. The contribution is indicated using an arbitrary scale from black (no intensity contribution) to white (maximum intensity contribution). There exists a good correlation between the model data and the experimental data for all three PBO fibre types. This indicates the applicability of such a model for the analysis of RFT. The close approximation between the model and experimental data also shows that the previously suggested hypothesis that there exists a radial orientation of the *a*-unit cell axis about the fibre axis is valid [1]. The iterated FWHM values for the modelled distributions in RFT and other model parameters are collected in Table 1.

The modelling results further indicate that the degree of rotational disorder (distribution in RFT) is in the same fibre order as tensile modulus and axial crystalline domain orientation [11,13]. Thus, PBO AS exhibits the lowest degree of radial orientation (lowest RFT FWHM) and HM+ the highest. It is interesting that heat-treatment and non-aqueous coagulation both result in an increase in the degree of crystalline domain orientation both in the fibre axis direction and about the fibre axis [13]. Thus orientation improvements arising through processing occur uniaxially.

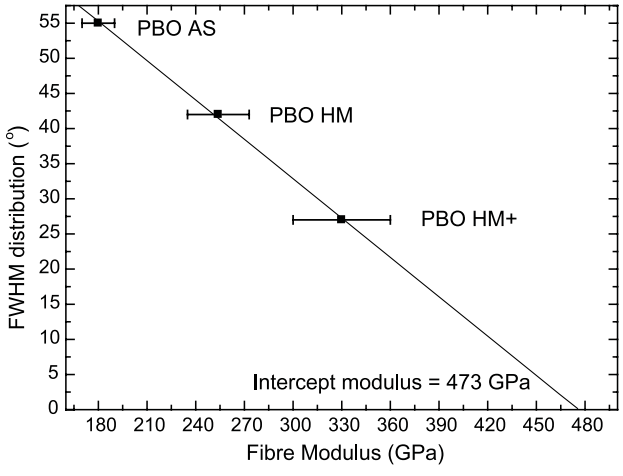

Fig. 7. Extrapolation of modulus to zero FWHM based on modelled data.

The FWHM value of 27° obtained for PBO HM+ in this study is similar to the value of 28° determined in a previous study of PPTA using a similar method [19]. This may indicate that despite the lack of inter-chain bonding in PBO [24,25] the HM+ fibre has a level of radial crystallite orientation similar to PPTA which has hydrogen bonding between chains [26]. A similar study on Kevlar[49] has reported a significantly lower FWHM value of 56° [27], similar to the value of 55° in this study for PBO AS. The differences between the FWHM values in the distribution in RFT for PPTA reported in these previous studies may be due to the use of different PPTA fibre varieties.

It has been reported previously that the HM+ fibre has the most homogeneous structure and AS the least homogeneous [1,10]. This difference between the PBO fibre types is thought to be partially responsible for the differences in crystalline domain orientation and tensile modulus [1,10]. It may therefore be hypothesised that the degree of RFT is also related to the level of homogeneity within the fibre structure. If this hypothesis is true, then it follows that perfect RFT should correspond to a perfectly homogeneous fibre structure. This is shown in the idealised model (Fig. 3). Thus such a perfectly homogeneous fibre should also exhibit an optimum tensile modulus, corresponding to the crystal modulus value.

By plotting the relationship between the FWHM in RFT against the fibre modulus of each fibre type, an extrapolation of modulus to zero FWHM can be performed. This is an extrapolation of modulus to that of a perfectly homogeneous fibre. This requires an assumption that the degree of RFT is related to the degree of fibre homogeneity. The result of this extrapolation is shown in Fig. 7. The extrapolated modulus of 473 GPa agrees favourably with the crystal modulus value reported for PBO HM of 474 GPa [11]. This therefore supports the hypothesis that the degree of rotational orientation in RFT is related to fibre homogeneity.

4. Conclusions

A micro-focus synchrotron beam can be used to investigate RFT in PBO fibres through variations in equatorial reflection intensity across the fibre. A straightforward model allows the degree of radial fibrillar texturing to be determined in terms of a Gaussian FWHM. The use of a

PBO model with the *a*-unit cell axis oriented radially about the fibre axis supports the findings of previous studies [1].

From modelling, the distribution in RFT is found to be in the same fibre order as tensile modulus for PBO. Both heat-treatment and the modified non-aqueous coagulation of the HM+ fibre type decrease the distribution in RFT. This is indicated by the lower FWHM required to fit the experimental results for the PBO HM and HM+ fibre types. These findings are similar to those of axial crystalline domain orientation [13].

Tensile modulus improvements during fibre processing are thought to result through an increase in fibre homogeneity. It may therefore be hypothesised that the distribution in RFT is related to the degree of fibre homogeneity. An extrapolation of PBO fibre modulus to zero RFT FWHM yields a modulus close to the crystal modulus value. The extrapolated result therefore supports this hypothesis.

Acknowledgements

The authors thank Toyobo (Japan) for the supply of PBO fibres for this study. The assistance of colleagues from the Manchester Materials Science Centre is also acknowledged, as is the EPSRC for funding of this project. Assistance received from staff on the ID13 beamline of the ESRF is greatly appreciated, in particular S. V. Roth and M. Burghammer.

References

[1] Kitagawa T, Murase H, Yabuki K. J Polym Sci: Polym Phys 1998; 36(1):39–48.
[2] Day RJ, Robinson IM, Zakikhani M, Young RJ. Polymer 1987; 28(11):1833–40.
[3] Young RJ, Day RJ, Zakikhani M. J Mater Sci 1990;25(1A):127–36.
[4] Wolfe JF. Polybenzothiazoles and polybenzoxazole. In: Mark HF, editor. Encyclopedia of polymer science and engineering. New York: Wiley; 1988. p. 601.
[5] Arnold Jr FE. Rigid-rod polymers and molecular composites. In: Hergenrother PM, editor. Advances in polymer science: high performance polymers. Berlin: Springer; 1994. p. 259.
[6] Kumar S. Ordered polymer fibres. In: Lee SM, editor. Enyclopedia of composites. New York: VCH Publishing; 1990. p. 51.
[7] Kitagawa T, Yabuki K, Young RJ. Polymer 2001;42(5):2101–12.
[8] Ledbetter HD, Rosenberg S, Hurtig CW. Mater Res Soc Symp 1989; 134:253.
[9] Choe EW, Kim SN. Macromolecules 1981;14(4):920–4.
[10] Kitagawa T, Ishitobi M, Yabuki K. J Polym Sci: Polym Phys 2000; 38(12):1605–11.
[11] Davies RJ, Montes-Morán MA, Riekel C, Young RJ. J Mater Sci 2001;36(13):3079–87.
[12] Montes-Morán MA, Davies RJ, Riekel C, Young RJ. Polymer 2002; 43(19):5219–26.
[13] Davies RJ, Montes-Morán MA, Riekel C, Young RJ. J Mater Sci 2003;38(10):2105–15.
[14] Riekel C, Cedola A, Heidelbach F, Wagner K. Macromolecules 1997; 30(4):1033–7.
[15] Roth S, Burghammer M, Janotta A, Riekel C. Macromolecules 2003; 36(5):1585–93.
[16] Krause SJ, Haddock TB, Vezie DL, Lenhert PG, Hwang WF, Price GE, Helminiak TE, O'Brien JF, Adams WW. Polymer 1988; 29(8):1354–64.
[17] Martin DC, Thomas EL. Macromolecules 1991;24(9):2450–60.
[18] Paris O, Loidl D, Muller M, Lichtenegger H, Perterlik H. J Appl Crystallogr 2001;34:473–9.
[19] Riekel C. Rep Prog Phys 2000;63(3):233–62.
[20] Davies RJ, Eichhorn SJ, Riekel C, Young RJ. Polymer 2004;45(22): 7693–704.
[21] Hammersley AP, Svensson SO, Thompson A. Nucl Instrum Methods Phys 1994;346(1–2):312–21.
[22] Hammersley AP, Svensson SO, Thompson A, Graafsma H, Kvick Å, Moy JP. Rev Sci Instrum 1995;66(3):2729–33.
[23] Fratini AV, Lenhert PG, Resch TJ, Adams WW. Mater Res Symp Proc 1989;134:431.
[24] Tomlin DW, Fratini AV, Hunsaker M, Adams WW. Polymer 2000; 41(25):9003–10.
[25] Hageman JCL, Van der Horst JW, Groot RA. Polymer 1999;40(5): 1313–23.
[26] Klop EA, Lammers M. Polymer 1998;39(24):5987–98.
[27] Riekel C, Dieing T, Engstrom P, Vincze L, Martin C, Mahendrasingam A. Macromolecules 1999;32(23):7859–65.